Reaction of amorphous Ni-W and Ni-N-W films with substrate silicon

M. F. Zhu,[a] I. Suni,[b] and M-A. Nicolet
California Institute of Technology, Pasadena, California 91125

T. Sands
Materials and Molecular Research Divison, Lawrence Berkeley Laboratory, Berkeley, California 94720

(Received 2 April 1984; accepted for publication 19 June 1984)

Amorphous films of Ni-W and Ni-N-W were deposited on single-crystal silicon with discharge gases of Ar or Ar + N_2 by rf cosputtering of Ni and W. The reaction of these Ni-W and Ni-N-W films with the Si substrate were studied in the temperature range of 450–750 °C by a combination of backscattering spectrometry, x-ray diffraction, cross-sectional transmission electron microscopy, and resistivity measurements. Films with composition $Ni_{36}W_{64}$ are stable below 500 °C. NiSi and $NiSi_2$ form at 500 °C, and WSi_2 forms rapidly in the temperature range of 625–650 °C. The nickel silicide forms adjacent to and within the silicon, while the outer layer becomes a mixture of WSi_2 and $NiSi_2$. The morphologies of the reacted layers are revealed by cross-sectional transmission electron microscopy. The crystallization temperature of amorphous $Ni_{36}W_{64}$ films on SiO_2 is near 650 °C also. Adding nitrogen to form amorphous $Ni_{30}N_{21}W_{49}$ films lowers the crystallization temperature, but raises the reaction temperature with Si to 750 °C.

I. INTRODUCTION

Polycrystalline binary alloys of near-noble refractory metals have attracted interest for shallow silicide contacts in very-large-scale-integrated (VLSI) circuits.[1–4] These investigations indicate that the initial reaction proceeds by silicide formation and phase separation and is determined by the compound with the lowest formation temperature. However, little is known about the behavior of *amorphous* binary alloys in contact with silicon. Investigations of amorphous metallic films and comparison with polycrystalline films broadens the understanding of multilayer metallization reactions. In the recent past, amorphous metallic alloys have attracted special attention as primary metallization and as diffusion barriers for high temperature device applications because of their low atomic diffusivity.

Sputtered amorphous films of Nb-Ni, Mo-Ni, Si-W, and Si-Mo have been studied by Wiley *et al.*[5] Amorphous Fe-W[6] and Ni-Mo[7] films as diffusion barriers between multilayer metallizations on silicon demonstrate good electrical and thermal stability. The Ni-W system was chosen for this study because it is similar to the Ni-Mo system, but W has a higher silicide formation temperature than Mo.[8,9] Both systems fulfill the same basic requirements for amorphous phase formation with different crystal structures and atomic sizes of the constituent elements.

It is well known that the nitrides of the early transition metals, such as TiN, are quite stable.[10] In an attempt to improve the stability of amorphous Ni-W films as a diffusion barrier, nitrogen has been introduced into the Ni-W film during deposition. Although the crystallization temperature is thereby lowered, the thermal stability of the Ni-N-W films in contact with silicon is markedly improved.

II. EXPERIMENTAL PROCEDURES

A. Sample preparation

The amorphous Ni-W films were obtained by cosputtering Ni and W on ⟨100⟩ oriented 1–10-Ω cm Si substrates at room temperature and on SiO_2 substrates. The sputtering was carried out in a radio frequency (rf) planar magnetron sputtering system equipped with an oil diffusion pump. A bare circular W cathode partially covered with a Ni mask was used as the sputtering source. The initial vacuum before the depositions was in the low 10^{-6} Torr range. Pure Ar gas or a mixture of 90% Ar and 10% N was introduced into the evacuated sputtering chamber. During sputtering, the chamber pressure was 10 mTorr and the incident rf power was 300 W. To obtain a uniform film, the substrate table was rotated under the target at a rate of 1 rpm. The average deposition rate on the sample was 40 Å/min for Ar and 50 Å/min for 90% Ar + 10% N_2. The Ni and W concentrations were varied by using different Ni masks or by adding N_2.

Prior to loading the sputtering chamber, each bare Si substrate passed through organic cleaning and etching in dilute HF for 10 sec to remove residual silicon dioxide. After the deposition, the samples were annealed at various temperatures in a vacuum furnace for 30 min at a pressure below 5×10^{-7} Torr. To determine the concentration of N, the amorphous Ni-N-W film was simultaneously deposited on a carbon substrate in the same run for subsequent backscattering spectrometry (BS) analysis.

B. Sample characterization

2-MeV $^4He^+$ BS was used to determine the depth profiles of the elements in each film, to estimate the layer thickness by evaluating the number of atoms per unit area of the amorphous Ni-W and Ni-N-W films, and to monitor the interfacial reactions after thermal treatment. The backscattered ions were detected at a 170° scattering angle and

[a] Permanent address: Graduate School, University of Science and Technology of China, Beijing, China.
[b] Permanent address: Semiconductor Laboratory, Technical Research Centre of Finland, Otakaari 5A, SF-02150 Espoo 15, Finland.

 0021-8979/84/222740-06$02.40

analyzed in multichannels of 2.94 keV per channel. Phases and structures of the film on Si and SiO_2 were identified by glancing angle x-ray diffraction (Read Camera) after each annealing treatment. The samples analyzed by x-ray and BS to correlate the film structure with the reaction kinetics were deposited in the same run and annealed simultaneously. The surface topology was observed by optical microscopy. The reactions between the amorphous film and Si and the crystallizations of the amorphous film after high temperature annealing were monitored by four-point probe measurements of sheet resistance at room temperature for samples annealed in the temperature range of 350–800 °C.

Film morphologies and the lateral distributions of phases were determined by cross-sectional transmission electron microscopy (XTEM) and diffraction. Specimens for XTEM were prepared by bonding cleaned and oriented samples face-to-face, followed by mechanical polishing, and finally, ion milling. Argon ion milling was performed with a 5-keV beam, a specimen current of 20 μA, and a specimen tilt of 16°. The specimen stage was cooled with LN_2 to limit beam heating effects. Specimens were observed in a JEOL 200-CX TEM with a high-resolution pole piece ($c_s \cong 1.2$ mm). Axial high-resolution images in ⟨110⟩ zone-axis orientation were recorded with an objective aperture which included nine beams. The high-resolution images shown below were taken near the Scherzer defocus condition (~ 700 Å).

III. RESULTS

A. Interaction between amorphous Ni-W films and Si

From BS data, the average composition of the films is $Ni_{36}W_{64}$. Assuming that the density of the amorphous layer is a linear combination of the elemental atomic densities (Vegard's law), the thicknesses of the films were evaluated to be 400–1000 Å. The as-deposited films were amorphous as confirmed by x-ray diffraction.

The BS spectra of a $Ni_{34}W_{64}$ sample, as-deposited and annealed at 625 and 650 °C for 30 min, are shown in Fig. 1. The BS result indicates no detectable interdiffusion below 500 °C. Beginning at about 500 °C, a movement of Ni into the Si is perceptible. At 600 °C, the average concentration of Ni at 100 nm below the Si interface is on the order of a few percent. A corresponding movement of W into Si would be readily detected, but was not. There is no visible penetration of Si into the amorphous film, but the sensitivity to Si there is low. In Fig. 1, this deep penetration of Ni into Si is clearly seen in the spectrum taken after a 625 °C annealing.

The total amount of Ni that penetrates into the Si as a function of annealing time was studied by taking the difference of the counts in the Ni signals before and after annealing at 500 °C. For this purpose, only those counts were considered that corresponded to Ni atoms beyond a fixed depth of 50 nm below the Si/film interface. The result at 500 °C is plotted in Fig. 2. It can be seen that this total amount of Ni increases linearly with time. This linearity was observed regardless of the depth beyond which the Ni atoms were counted.

This penetration of Ni into Si at 500 °C has been investigated in detail by XTEM. The images reveal the presence of pyramidal penetrations after 30 min. The high-magnifications image in Fig. 3 shows that these pyramids have sharp {111} facets. The lack of detectable extra spots in the electron diffraction pattern and the apparent continuity of the fringes within the pyramids suggest that these penetrations are epitaxial $NiSi_2$. This interpretation is supported further in the next section. The light band visible in Fig. 3 at a depth

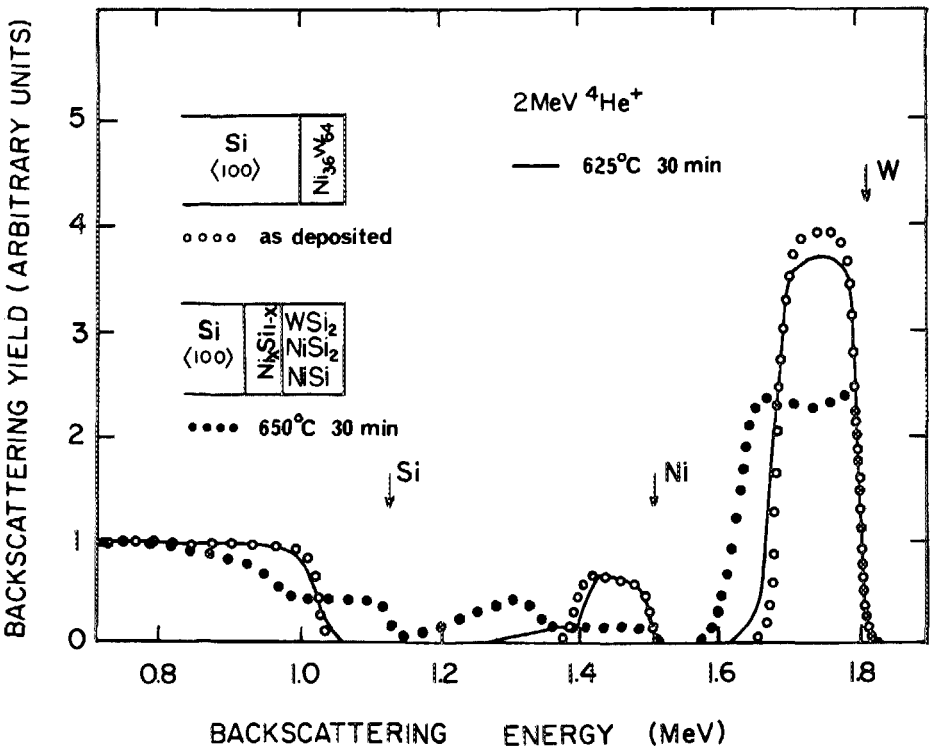

FIG. 1. Backscattering spectra of 800-Å-thick amorphous $Ni_{36}W_{64}$ films on ⟨100⟩ Si, as-deposited (open circles, O) and annealed for 30 min at 625 °C (continuous line, ———), 650 °C (filled circles, ●). The detection angle is 170°. The presence of NiSi in the outer layer of the annealed sample is probable, although only $NiSi_2$ and WSi_2 have been proved.

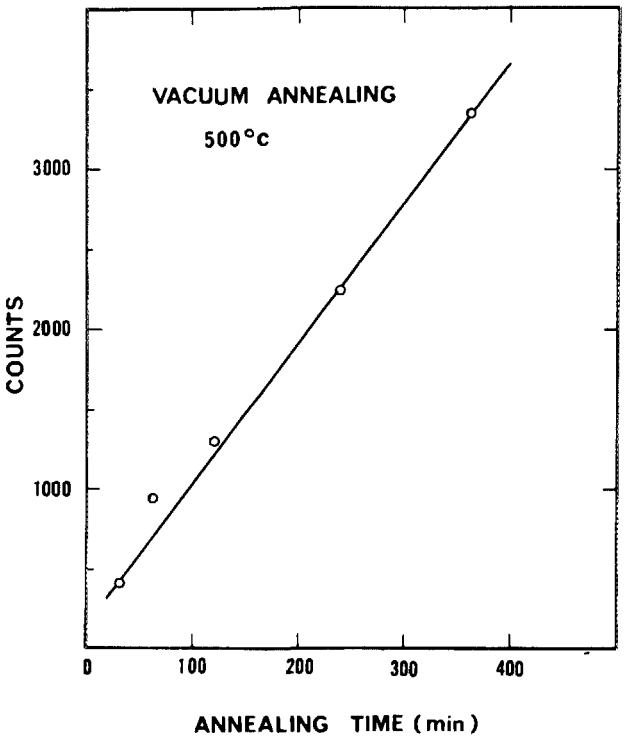

FIG. 2. Time dependence of amount of nickel in silicon at 500 °C.

of ~240 Å is probably a thin oxide layer which was present on the substrate surface during deposition. This thin layer may affect the nickel silicide reactions (see discussion).

A large portion of the Ni which penetrates into the Si substrate is in the form of orthorhombic NiSi precipitates (Fig. 4). Since the size and density of $NiSi_2$ pyramids does not change noticeably between 30-min and 2-h annealing time, these NiSi precipitates account for most of the penetrating Ni observed by BS in Fig. 2 as the annealing time increases at 500 °C.

Figure 1 also shows that at 625 °C, in addition to the deep penetration of Ni into Si, the Ni, Si, and W signals change visibly at the interface with Si. At 650 °C, that interaction completely dominates the outcome. An outer layer of fairly uniform composition containing Si, Ni, and W in the approximate ratios of 66 : 7 : 27 forms. X-ray diffraction analysis of this sample reveals the presence of polycrystalline WSi_2. Assuming that all W is in this form, the atomic composition in that outer layer is consistent with a film of WSi_2 and $NiSi_2$ in a molecular ratio of 6.3 : 1.4, meaning that only

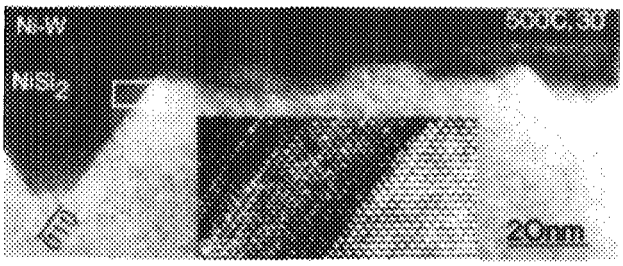

FIG. 3. High-resolution XTEM micrograph of interfacial region after annealing at 500 °C, 30 min. Image characteristics of penetration pyramid at left strongly suggests $NiSi_2$ phase. Light band is possibly due to thin interfacial oxide which is at depth of 240 Å from surface.

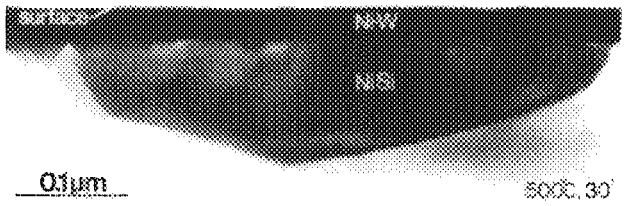

FIG. 4. XTEM image of NiSi precipitate formed during annealing of 400 Å thick $Ni_{36}W_{64}$ layer at 500 °C for 30 min. The metallic layer retains amorphous character at this temperature.

~1/3 of the Ni is contained in that layer. The rest of the Ni reacts with Si and is located preferentially between this outer layer and the Si substrate (see Fig. 1). The x-ray pattern contains lines in addition to those of WSi_2, but they are too weak and incomplete in number to positively identify them as a Ni silicide.

The XTEM micrograph in Fig. 5 reveals the morphology of a $Ni_{36}W_{64}$ film annealed at 650 °C for 30 min. Reaction pits are visible at the surface above areas of deep intrusions of NiSi. The crystallographic relationship between this NiSi and the ⟨100⟩ Si substrate, as determined by electron diffraction and high resolution TEM (not shown) is {111} Si~‖{010} NiSi and {112} Si~‖{101} NiSi. The lower symmetry of the NiSi is demonstrated by the observation that the projection of the NiSi intrusion in the ⟨110⟩ Si direction appears either as triangular (e.g., Fig. 4) or rectangular (e.g., right side of Fig. 5) in form, suggesting a troughlike shape for these NiSi precipitates. The slanted sides of the trough are approximately parallel to {111} Si planes.

The morphology of the interface between Si and the mixed Ni-W-Si layer in a region between NiSi protrusions is shown in Fig. 6. In agreement with the x-ray results (Sec. III B), the layer is found to be polycrystalline. The areas with nearly vertical fringes at the interface correspond to grains with preferred orientations. The nearly vertical fringes have a spacing of 3.98 ± 0.05 Å corresponding to the (002) planes of WSi_2 (the 001 reflection is kinematically forbidden) in agreement with the x-ray results.

B. Crystallization of amorphous $Ni_{36}W_{64}$ films on SiO_2

Accompanying the interfacial reaction at the high annealing temperature is the crystallization of the amorphous Ni-W film that occurs. X-ray diffraction of a $Ni_{36}W_{64}$ film on Si indicates that the film stays amorphous upon annealing up to 600 °C. At 625 °C, two weak W lines could be observed; on SiO_2, no lines could be detected. At 650 °C, the film is

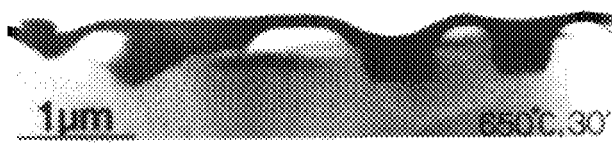

FIG. 5. XTEM micrograph of 800 Å thick $Ni_{36}W_{64}$ film after annealing at 650 °C for 30 min. A 1000-Å-thick surface layer has undergone crystallization and silicide formation. The deep penetrations below the reaction pits are NiSi.

FIG. 6. High-resolution XTEM micrograph of interface between 1000-Å-thick surface layer and Si substrate after heat treatment at 650 °C for 30 min. Note polycrystalline nature of surface layer. Nearly vertical fringes correspond to (002) planes of WSi_2 particles in contact with silicon at interface.

polycrystalline on either substrate, as indicated by WSi_2 and W lines, respectively.

The crystallization has also been monitored by sheet resistance measurements at room temperature. The resistivity of as-deposited amorphous $Ni_{36}W_{64}$ films is 170 $\mu\Omega$ cm. Figure 7 shows the sheet resistance ratio between annealed and unannealed samples as a function of annealing temperature for films on Si and SiO_2. On SiO_2, the ratio is temperature independent and remains at unity below 600 °C. Starting at 650 °C, the sheet resistance decreases rapidly. On Si, the sheet resistance decreases slightly, but distinctly already below 600 °C, and then drops rapidly above 625 °C. The onset of the fast decrease is clearly associated with the crystallization of the film as indicated by the x-ray analysis.

C. Amorphous Ni-N-W films

The average composition of the as-deposited Ni-N-W films is $Ni_{30}N_{21}W_{49}$. The film thickness was estimated to be 1100 Å. The resistivity of the amorphous film is 260 $\mu\Omega$ cm. By x-ray diffraction, the as-deposited films are amorphous.

By BS analysis, a $Ni_{30}N_{21}W_{49}$ film does not detectably react with Si in 30 min below 725 °C. At 750 °C, the layer reacts, and does so laterally more nonuniformly than without nitrogen. X-ray diffraction provides the interesting result that the amorphous $Ni_{30}N_{21}W_{49}$ film crystallizes before it reacts with the Si substrate. After annealing at 600 °C, a number of lines indicate that W has formed W_2N, and perhaps WN. The W_2N lines intensify with increasing annealing temperature up to 700 °C. When WSi_2 lines appear, the diffraction pattern of W_2N weakens.

The normalized sheet resistance at room temperature as a function of the annealing temperature for 30-min duration is shown in Fig. 8 for films deposited on Si and SiO_2, respectively. The results differ generally from those of Fig. 7 in the temperature range of 500–700 °C. The sheet resistance ratio of films on SiO_2 and Si first increase to a peak value of 1.3 at 600 °C before it decreases beyond that point.

IV. DISCUSSION

A. Silicide formation and phase separation

The reactions observed can be divided into two stages. In the first stage at low temperatures (500 °C for $Ni_{36}W_{64}$), Ni penetrates into the Si substrate. In the second stage, which begins at 625–650 °C for $Ni_{36}W_{64}$, the reactions between W, Ni, and Si involve the incorporation of Si into the surface layer.

At 500 °C, two types of Ni penetrations are observed. First, tetrahedral pyramids of $NiSi_2$ with sharp {111} facets form in the Si near the interface (Fig. 3). This transformation does not require the diffusion of Si, but rather the slight rearrangement of the Si unit cell and the incorporation of Ni in interstitial positions. This mode of nickel silicide growth is well established. On clean Ni-Si interfaces, $NiSi_2$ does not generally form at 500 °C when the supply of Ni is unlimited.[11] The availability of Ni is clearly locally limited in the present case, quite probably by the presence of a thin oxide layer on the original Si substrate, but perhaps also by the reduced concentration of Ni in the mixed Ni-W layer. It is also possible that even without impurities an interfacially controlled reaction between an amorphous binary alloy and Si is laterally unstable. Second, large NiSi precipitates are observed. Their localized growth must again be understood in terms of a laterally irregular supply of Ni. These precipi-

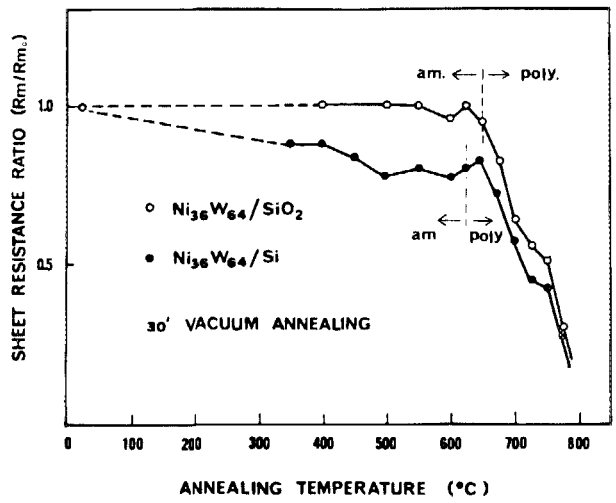

FIG. 7. Ratio of the sheet resistance for amorphous $Ni_{36}W_{64}$ films deposited on Si and SiO_2 after (R_m) and before (R_{m0}) vacuum annealing for 30 min as a function of annealing temperature.

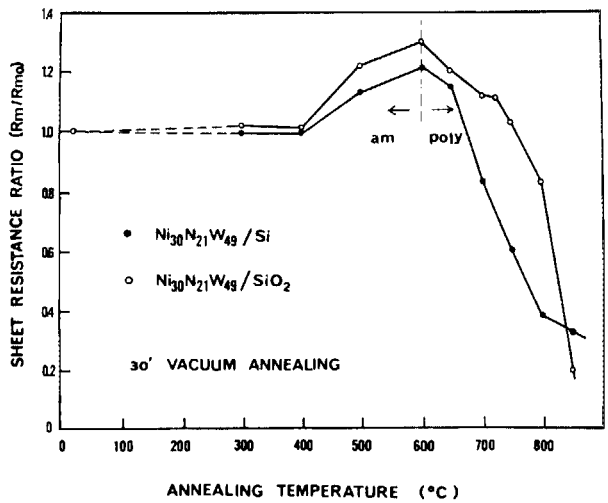

FIG. 8. Ratio of the sheet resistance for amorphous $Ni_{30}N_{21}W_{49}$ film deposited on Si and SiO_2 after (R_m) and before (R_{m0}) vacuum annealing for 30 min as a function of annealing temperature.

tates account for the linear time dependence of Ni penetration measured by BS (Fig. 2). Their growth is presumably limited by the silicide-metal interface. Both types of Ni penetration occur without noticeable changes in the bulk of the film whose composition remains unchanged and whose structure stays amorphous. The existence of this deep Ni penetration at a temperature at which the film remains amorphous has a corollary for diffusion barrier applications. A high crystallization temperature is an important criterion for the selection of amorphous alloys in this application. But the amorphous state of the film in itself evidently does not assure the stability of the interface. The study of interfacial reactions of amorphous metallic films with single crystalline substrates (or with polycrystalline overlayers) thus becomes a subject of particular interest.

When the film reacts at high annealing temperatures (625–650 °C), the BS results demonstrate that the Ni reacts preferentially near the Si interface, while W remains in the outer layer. Such phase separations have been reported in earlier studies and are common for polycrystalline binary alloys or bilayers of near-noble and refractory metals.[3,12] The compounds observed are WSi_2 and $NiSi_2$, which are those expected from the binary phase diagram of Ni and W in the presence of excess Si. In fact, the Ni silicide and WSi_2 are not separated completely. Some $NiSi_2$ remains in the surface layer. The evidence contaned in Figs. 1–6 reveals that at least three effects enter in the detailed interpretation of phase separation: (i) the laterally nonuniform nature of the reactions (that subsequently leads to a vertical *and* lateral flow of atoms), (ii) the interfacial limitations of reactions, and (iii) the identity of the dominant moving species in the phases formed. It is conceivable that these effects are important also in the phase separation of polycrystalline alloy films. The detailed explanation of the phenomenon is obviously complicated.

B. Crystallization of amorphous $Ni_{36}W_{64}$ and $Ni_{30}N_{21}W_{49}$ layers

For amorphous $Ni_{36}W_{64}$ films, the sheet resistance on Si and SiO_2 indicate that the strong reaction with Si sets in close to the crystallization temperature of the film on SiO_2. Apparently, the macroscopic penetration of Si into the W and of Ni into the Si set in as the film crystallizes. Both the crystallization and the silicide reaction processes lead to a rapid decrease in the sheet resistance of the film. On Si, there is an additional slight lowering of the sheet resistance below the reaction at 625–650 °C which we attribute to the interfacial penetration of Ni into the Si, and the formation of NiSi and $NiSi_2$ while the bulk of the film remains unaltered. $I(V)$ measurements of Schottky barrier diodes made of a similar film on n-type ⟨100⟩ Si show a degradation of the diode characteristics in the same temperature range ($\sim$500 °C).[13]

Adding N into the amorphous Ni-W film significantly alters the properties of the film. On the SiO_2, as the film crystallizes its sheet resistance increases. We attribute this rise to the formation of polycrystalline W_2N, whose presence is indicated by x-ray diffraction. The resistivity of W_2N ($\sim$1650 $\mu\Omega$ cm)[14] is about six times that of the amorphous $Ni_{30}N_{21}W_{49}$ film (270 $\mu\Omega$ cm). The subsequent rapid decrease of the sheet resistance with increasing temperature of annealing in Fig. 8 can be explained by the formation of connected metallic paths. That the crystallization is not observed below 600 °C by x-ray diffraction while the sheet resistivity rises already above 400 °C may be attributed to the fine-grained structure of the initial crystalline phase. Nucleation and growth may thus actually occur below the indicated crystallization temperature of 600 °C. On Si, in contrast to the nitrogen-free layer, the $Ni_{30}N_{21}W_{49}$ film does not react with the substrate Si upon crystallization. A significant reaction sets in only at 750 °C, although crystallization occurs at 600 °C or lower. The amorphous or crystallized $Ni_{30}N_{21}W_{49}$ film is thus more stable against reactions with the Si substrate than the amorphous $Ni_{36}W_{64}$ film without N. The reduced reaction of Ni in the nitrogen containing film is unlikely to be the result of the binding of Ni by N, since Ni does not form stable nitrides at these elevated temperatures. Rather, the enhanced stability may be the result of a kinetic barrier formed by the stable W_2N. Detailed XTEM studies are very desirable to clarify this question.

V. CONCLUSION

The results of this study, in combination with previous investigations of amorphous Mo-Ni and Fe-W films on Si,[6,7] show that above their crystallization temperature, the behavior of amorphous binary alloys on Si is qualitatively similar to that of corresponding polycrystalline binary alloys. Below the crystallization temperature, a detailed study reveals the existence of interfacially controlled, and laterally confined reactions of one metallic constituent of the film (Ni) with Si. The cause of this lateral irregularity remains unspecified, but could be attributed to interfacial impurities or inherent instabilities in interfacially controlled reactions.

Although undesirable in practice, these reactions also indicate that an amorphous metallic binary alloy film reacts much more sluggishly with Si than the crystalline counterpart. This fact is evidenced by the elevated annealing temperatures that are required to induce these reactions. The direct experimental proof of the statement—a parallel treatment of samples with the same alloy film in either amorphous or crystalline form—remains to be given.

For applications to Si device contacting, this reduced reactivity of amorphous films is noteworthy. Possible ways to suppress or circumvent the undesirable local reactions below the crystallization temperature are to replace Ni by an element with a higher silicide formation temperature; use a buffer layer (e.g. NiSi) between the amorphous film and the Si substrate; ternary amorphous films (e.g., Ni-N-W); and multilayered amorphous films. In view of the practical interest, these possibilities will no doubt all be tested, and soon.

ACKNOWLEDGMENTS

The authors would like to thank Dr. M. Van Rossum and Eric T-S. Pan for x-ray diffractions. One of the authors (T. S.) wishes to acknowledge Professor J. Washburn, Professor R. Gronsky, and Dr. J. Mazur of Lawrence Berkeley Laboratory, University of California, Berkeley, for useful discussions. The completion of this work was financially supported at Caltech by the National Aeronautics and Space

Administration and monitored by the Jet Propulsion Laboratory, California Institute of Technology (D. Burger).

[1]J. W. Mayer, S. S. Lau, and K. N. Tu, J. Appl. Phys. **50**, 5855 (1979).
[2]K. N. Tu, W. N. Hammer, and J. O. Olowolafe, J. Appl. Phys. **51**, 1663 (1980).
[3]K. N. Tu, J. Vac. Sci. Technol. **19**, 725 (1980).
[4]A. Appelbaum, M. Eizenberg, and R. Brener, Vacuum **33**, 227 (1983).
[5]J. D. Wiley, J. H. Perepezko, J. E. Nordman, and Kang-Jin Guo, IEEE Trans. Ind. Electron. Control Instrum. **IE-29**, 154 (1982).
[6]I. Suni, M-A. Nicolet, C. S. Pai, and S. S. Lau, Thin Solid Films **107**, 73 (1983).
[7]K. T-Y. Kung, I. Suni, and M-A. Nicolet, J. Appl. Phys. **55**, 3882 (1984).
[8]R. W. Bower and J. W. Mayer, Appl. Phys. Lett. **20**, 359 (1972).
[9]B. Oertel and R. Sperling, Thin Solid Films, **37**, 359 (1972).
[10]C. W. Nelson, *Proceedings of the International Symposium on Hybrid Microelectronics*, September 29–October 1, 1969, Dallas, Texas (International Society of Hybrid Microelectronics, Montgomery, Alabama, 1969), p. 413.
[11]C. Canali, F. Catellani, G. Ottaviani, and M. Prudenziati, Appl. Phys. Lett. **33**, 187 (1978).
[12]G. Ottaviani, K. N. Tu, J. W. Mayer, and B. Y. Tsaur, Appl. Phys. Lett. **36**, 331 (1980).
[13]M. F. Zhu, I. Suni, and M-A. Nicolet (unpublished).
[14]G. V. Samsonov, Sov. Phys. Tech. Phys. **1**, 695 (1967).